

Model of overdamped motion of interacting magnetic vortices through narrow superconducting channels

Petruccio Barrozo,^{1,2} André A. Moreira,¹ J. Albino Aguiar,² and José S. Andrade, Jr.^{1,3}

¹*Departamento de Física, Universidade Federal do Ceará, 60455-760 Fortaleza, CE, Brazil*

²*Departamento de Física, Universidade Federal de Pernambuco, 50670-901 Recife, PE, Brazil*

³*National Institute of Science and Technology for Complex Systems, Xavier Sigaud 150, 22290-180 Rio de Janeiro, RJ, Brazil*

(Received 28 August 2009; published 28 September 2009)

The microscopic description of several physical systems can be successfully accomplished in terms of the overdamped flow approximation. It is under this broad framework that we investigate the flow of interacting particles in overdamped motion through narrow and irregular channels. By direct comparison with results from molecular dynamics simulations, we show that the behavior of the overdamped system is fully compatible with a continuum coarse-grained model, described in terms of a nonlinear diffusion equation. Remarkably, our results reveal that even in such cases where only a few layers of particles move through the channel, it is possible to obtain a consistent description for the density profiles from the continuum model. Moreover, we demonstrate the general validity of our theoretical approach with results from extensive numerical simulations of different model systems, including the propagation of vortices in superconducting substrates, the movement of pedestrians through corridors, and the flow of colloidal particles in pores.

DOI: [10.1103/PhysRevB.80.104513](https://doi.org/10.1103/PhysRevB.80.104513)

PACS number(s): 74.78.Na, 45.70.Vn, 74.25.Qt

I. INTRODUCTION

A great deal of attention has been directed to the dynamics of interacting particles in confined geometries.¹ Important examples of such systems are colloidal suspensions,² charge density waves,³ ion channels,⁴ vortex dynamics in superconductors,⁵ and pedestrian traffic.⁶ These systems exhibit a remarkable variety of complex behaviors depending on particular conditions.^{7,8} Although many of the phenomena observed in such systems are related to the discrete nature of their constituents, a general macroscopic description could help model and predict the dynamics of large systems comprising many interacting particles. Under this framework, a continuum formulation based on a coarse-grained description of the motion of overdamped particles has been proposed in previous studies.^{9–11}

It is the aim of the present study to investigate the flow of interacting particles undergoing overdamped motion through narrow and irregular channels. In particular, we focus on the situation where there is an obstacle to the flow, being either an energy barrier or a constriction in the channel. Surprisingly, we observe that even in such confined geometries, the continuum approach can successfully describe the density profiles obtained from direct molecular dynamics simulations of distinct physical systems, including the propagation of vortices, colloidal particles and flow of pedestrians in narrow channels.

II. MODEL FORMULATION

Our theoretical approach is initially tested for flow of vortices through a superconducting substrate, although it is generally valid for any overdamped system. We therefore consider the following equation of motion:^{12–15}

$$\eta \mathbf{v}_i = \mathbf{F}_i^{pp} + \mathbf{F}_i^{ext} + \mathbf{F}_i^T, \quad (1)$$

where \mathbf{F}_i^{pp} represents the particle-particle interaction, \mathbf{F}_i^{ext} is the external force acting on every particle, and \mathbf{F}_i^T is

the thermal interaction. In the case of vortex lines, the effective viscosity η can be expressed in terms of material parameters, namely, $\eta = \Phi_0^2 d / 2\pi \xi^2 \rho_N$, where d is the sample thickness, ξ is the coherence length, ρ_N is the resistivity in the normal state, and $\Phi_0 = h/2e$ is the quantum of magnetic flux. The particle-particle interaction is given by $\mathbf{F}_i^{pp} = \sum_{j \neq i}^{N_p} f_0 K_1(r_{ij}/\lambda) \hat{\mathbf{r}}_{ij}$,^{16–19} where $\hat{\mathbf{r}}_{ij} = (\mathbf{r}_i - \mathbf{r}_j) / |\mathbf{r}_i - \mathbf{r}_j|$ is the unitary vector in the direction of the axis from vortex j to vortex i , $K_1(r_{ij}/\lambda)$ is the modified Bessel function, $f_0 = \Phi_0^2 d / 2\pi \mu_0 \lambda^3$ is the force strength, and λ is the London penetration length.

For completeness, we present here the reasoning behind the formulation of the continuum model.^{9,10} We start from the continuity equation for the local density of particles, $\partial \rho / \partial t = \nabla \cdot \mathbf{J} + k_B T \nabla^2 \rho$, where $\mathbf{J} = \rho \mathbf{v}$ is the particle current, \mathbf{v} is the local average velocity, and the second term on the right accounts for thermal diffusion. As expressed in Eq. (1), we should expect this velocity to depend on the drive from the external force and the particle-particle interaction. It has been shown^{9,10} that the particle-particle interaction can be associated with the local density gradient as $\langle F^{vv} \rangle = a \nabla \rho$, where the parameter a can be deduced from the microscopic particle-particle interaction as $a = 1/2 \int d^2 r \mathbf{F}(\mathbf{r}) \cdot \mathbf{r}$, which gives $a = d \Phi_0^2 / \mu_0 = 2\pi f_0 \lambda^3$ for the case of vortices.¹⁰ This expression, however, is valid only at relatively large density values, $\rho > \Phi_0 / \lambda^2$, and when the density gradient varies slowly $\nabla^2 \rho < \Phi_0 / \lambda^4$. Considering all these assumptions, we can now rewrite the continuity equation as

$$\eta \frac{\partial \rho(\mathbf{r}, t)}{\partial t} = \nabla \cdot [\rho(a \nabla \rho - \mathbf{F})] + k_B T \nabla^2 \rho(\mathbf{r}, t), \quad (2)$$

where we have reduced the notation by dropping the superscript of the external force.

In narrow channels, and neglecting shear effects with the channel walls, the velocity profile is weakly dependent of the transversal coordinate, unless close to geometrical

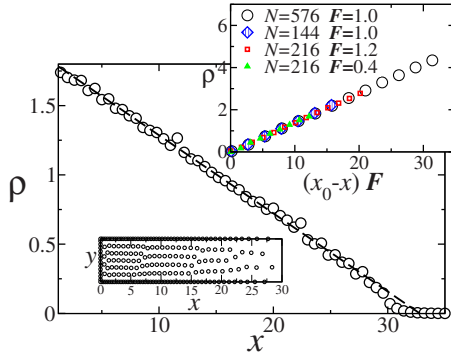


FIG. 1. (Color online) Linear density profile for a closed system consisting of N interacting vortices. The system is a channel of width $L=4.0\lambda$ with impenetrable walls (in every direction). An external force pushes the particles against the wall at $x=0$. We use molecular dynamics to simulate this system until the particles reach the stationary state of mechanical equilibrium, as shown in the inset at the bottom left. The main panel shows the density profile obtained at the final state for $N=576$ and $F=f_0$. The best linear fit to the data gives the position x_0 where the density vanishes, with the slope of the curve corresponding to F/a . The top-right inset shows the density profiles for different values of N and F . The slopes are all very close indicating a universal behavior of the curve a versus L (see Fig. 2).

obstacles.⁸ This fact allows us to adopt a simpler quasi-one-dimensional version of the transport model. Under steady-state conditions and neglecting thermal fluctuations, Eq. (2) reduces to

$$\rho \left(a \frac{d}{dx} \rho - F \right) = J, \quad (3)$$

where the conservation of the number of particles imposes the particle current J to be constant.

III. RESULTS

The first numerical experiment we perform is a finite narrow box closed in all four directions in which vortexes are pushed by an external force F against one of the lateral walls. In our idealized model, we treat the interaction with the channel walls as purely repulsive. Shear stress with the walls and bulk interactions with pinning centers are not included in our model system. In a closed box steady flux is not possible, $J=0$, and the solution of Eq. (3) is a linear profile, $\rho(x)=F/a(x-x_0)$, with x_0 being the position where the density vanishes, $\rho(x_0)=0$. In order to test the assumptions of our model, we perform molecular dynamics simulations for different values of N , F , and L until the system reaches mechanical equilibrium. Here, we estimate the density profile $\rho(x)$ as the local magnetic field averaged over time and normalized by the quantum of flux Φ_0 . From the slope of this profile (see Fig. 1), we can directly calculate the transport parameter a . As shown in Fig. 2, our results indicate that the behavior of a can be approximately described by a single curve expressing its dependence on L alone, over a broad range of N and F values.

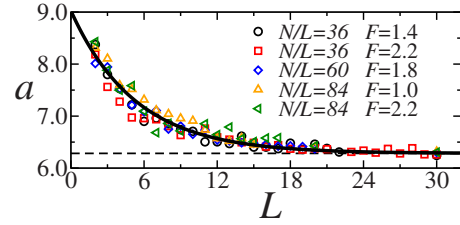


FIG. 2. (Color online) Variation in the parameter a against the width of the channel L . In order to obtain these results, we perform simulations in a confined system, as shown in Fig. 1, for several different conditions. The effective value of the parameter a is then obtained from the slope of the (linear) density profile. As the channel gets narrower, we observe deviations from the theoretical value, $a=2\pi(f_0\lambda^3/\Phi_0)$. The solid line indicates the least-squares fit to the points of the function $a(L)=[2\pi+c \exp(-bL)](f_0\lambda^3/\Phi_0)$, with $c=2.74$ and $b=0.19$. The parameter a is given in units of $f_0\lambda^3/\Phi_0$, and L in units of λ .

It is important to mention that, strictly speaking, the theoretical prediction $a=2\pi f_0\lambda^3/\Phi_0$ (the dashed line in Fig. 2) should be only valid for unconfined systems. In a confined channel, if the width of the channel is of the order of the characteristic length λ , the local density becomes somewhat smaller than the number of particles per unity of area. Such a discrepancy can be explained by the fact that vortices cannot leave the channel, while part of the magnetic field propagates out. This is equivalent to introducing an effective cross section for vortex transport that is greater than the width of the channel,^{20,21} therefore leading to an estimate of a that is larger than the value predicted theoretically.

We now try to extrapolate our findings from the static ($J=0$) to the dynamical case ($J\neq 0$). Our objective is to test if the values of a obtained from the static case can be used to describe particle flow driven by an external force through a long narrow channel and across an obstacle in the form of a potential jump ΔU as shown in Fig. 3.

In our simulations, we model this with a force given by $F^s=\Delta U/\delta$, where δ is the width of the region where the potential varies. The potential jump ΔU is given in units of $f_0\lambda$, the force is given in units of f_0 , and the length in units of λ . We adopt $\delta=0.1\lambda$, but the results become independent of

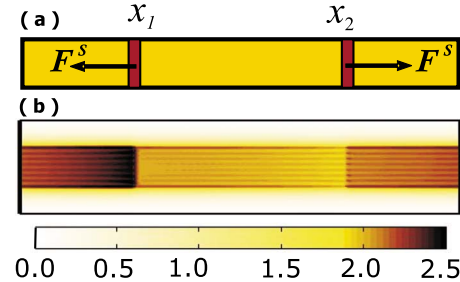


FIG. 3. (Color online) (a) Pictorial representation of the narrow channel with a potential barrier ΔU . The positions x_1 and x_2 , indicate the limits of the barrier where particles suffer the action of localized forces. In (b) we show a contour color plot of the average local density inside the channel. The corresponding color bar is below. This plot shows that inside the channel the local density depends weakly on the transverse coordinate.

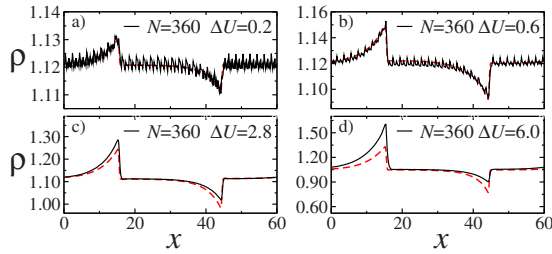


FIG. 4. (Color online) Density profiles for a channel with an obstacle to the flow, as described in Fig. 3. The particles move through a narrow channel, $L=2\lambda$, where we impose a potential barrier of amplitude $\Delta U=0.6$ from position $x_1=15\lambda$ to $x_2=45\lambda$. For simplicity, we impose periodic boundary conditions in the direction of the flow. When an external force $F=2.0f_0$ is applied to the system, the barrier introduces local forces, against the flow at x_1 , and in the direction of the flow at x_2 . The black (solid dark) lines are the results obtained from molecular dynamics simulations, while the red dashed lines correspond to the solutions from the numerical integration of the continuum model.

δ , as long as it is smaller than the typical distance between neighbor particles, $\delta < \ell$. In Figs. 4(a) and 4(b) we show the results of molecular dynamics simulations for small values of ΔU . It is seen that they are in good agreement with the numerical solution of Eq. (3), but for larger ΔU , as shown in Figs. 4(c) and 4(d), some deviations can be observed, especially in the vicinity of the positions x_1 and x_2 , where the particles have to overcome the potential barrier. The deviations for the cases of larger ΔU are expected, since the substrate force at the interface varies much faster than the distance between the particles, thus enhancing the effect of the discrete nature of the particles.

As an alternative approach to show the consistency between continuum model and molecular dynamics simulations, we can also solve analytically Eq. (3) separately for each section of the channel, before and after the obstacle, and account for the effect of the obstacle explicitly in the boundary conditions. In this case, the external force F , transversal section L , and current J , are constant in each section and the solution of Eq. (3) is given by,

$$\rho(x) = \frac{J}{F} \{1 + W[f(x)]\}, \quad (4)$$

where $f(x) = \exp(-1 + \rho_0 F / J + F^2 / a J x) (\rho_0 F / J - 1)$, ρ_0 is the value of the density in $x=0$ and $W(f)$ is the W-Lambert function, implicitly defined by the transcendental equation $x = W(x)e^{W(x)}$. By imposing conservation of the number of particles $N = \int L(x)\rho(x)dx$ and continuity of the current J , a relation between the values of ρ_0 for each section is obtained. Now we treat ρ_0 and J as free parameters and try to adjust the density profiles to Eq. (4).

The conservation of mass gives us relations for the parameters ρ_0 and J in each section, resulting in only two free parameters to the adjustment. The adjusting parameters are the density after the obstacle and the particle current. The best values obtained were $[\rho=1.121\lambda^{-2}, J=2.242f_0/(\eta\lambda^2)]$, $[\rho=1.120\lambda^{-2}, J=2.240f_0/(\eta\lambda^2)]$, $[\rho=1.112\lambda^{-2}, J=2.223f_0/(\eta\lambda^2)]$, and $[\rho=1.055\lambda^{-2}, J=2.109f_0/(\eta\lambda^2)]$, for

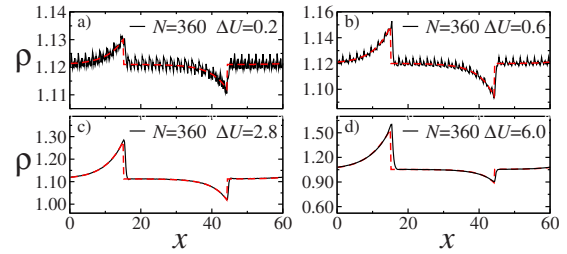


FIG. 5. (Color online) Adjust of the density profiles to the analytical solution Eq. (3). The best fit shown as the dashed red lines, follows closely the simulations data in all four cases.

$\Delta U=0.2, 0.6, 0.28$, and 6.0 , respectively. Moreover, the values for the current J obtained from the adjustment agree with the values obtained from the molecular dynamics up to the second decimal digit. The results obtained with this procedure, show in Fig. 5, are compared with the molecular dynamics simulation. Expectedly, it provides a superior description for $\rho(x)$ than the numerical solution of Eq. (3) in the absence of free parameters to fit (see Fig. 4), particularly for large values of ΔU . Moreover, the best values for the current density J are in good agreement with the values obtained from molecular dynamics simulations. The discrepancy observed in the results presented in Figs. 4(c) and 4(d) when compared to those shown in Figs. 5(c) and 5(d), can be attributed to the fact that the boundary conditions at the barrier interface are affected by the discrete nature of the particle system.

Next, we apply our coarse-grained approach to a narrow channel with a bottleneck, as shown in Fig. 6.

As before, we use molecular dynamics simulation to generate the density profiles, but now the general solution Eq. (4) is applied together with the continuity constraints at the channel junctions, $J_1 L_1 = J_2 L_2$ and $L_1 \int \rho_1(x)dx + L_2 \int \rho_2(x)dx = N$, where the indexes 1 and 2 correspond to the narrower and wider sections of the system, respectively. We emphasize here that the effective values for the parameter a used for each section are independently obtained from the numerical simulations with a closed box (see Fig. 2). Both the density profile from molecular dynamics and the best fit to the data of Eq. (4) are shown in Fig. 7. The excellent agreement substantiates the validity of our conceptual approach with a quasi-one-dimensional model, even in this case where the width of the channel is not constant. Note that, with this geometry, the external applied force produces a local increase in the particle density in the constricted region. This gives a way to control the local magnetic field density in superconductors with a transversal electric current.

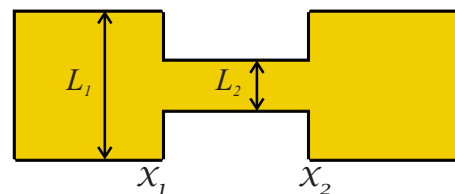


FIG. 6. (Color online) Pictorial representation of the channel with constriction employed in our simulations.

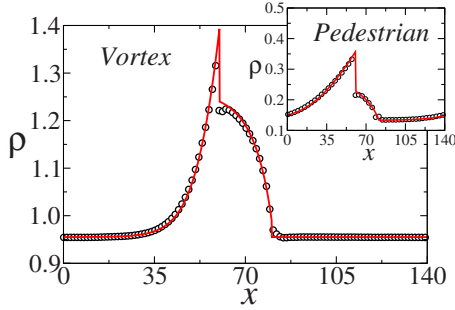


FIG. 7. (Color online) Density profile for systems of particles driven through a bottleneck. The main panel shows results concerning vortex dynamics, while the inset corresponds to the density profile of pedestrians modeled with an interaction given by Eq. (5). For the case of vortices, we use $N=1333$ particles driven by an external force $F=f_0$. The channel has a wide section 120λ in length by 10λ in width, and a narrow section of 20λ in length by 7.5λ in width. Periodic boundary conditions are applied in the direction of the flow. For the case of pedestrians, we use $N=312$ pedestrians with a natural velocity of 1 m/s. The flow of pedestrians is confined in a geometry with a section 10-m wide and 120-m long, with a bottleneck 2-m wide and 20-m long. In both cases, the results are in excellent agreement with the theoretical model Eq. (4) (solid red line). The adjusting parameters are the current J_1 and initial density ρ_1 in the narrow section. We obtain $J_1=1.262f_0/(\eta\lambda^2)$ and $\rho_1=1.24\lambda^{-2}$ for vortices, and $J_1=0.305\text{ s}^{-1}\text{ m}^{-1}$ and $\rho_1=0.22\text{ m}^{-2}$ for pedestrians.

The generality of our approach is illustrated here by applying the continuum model to other physical systems, namely, pedestrian dynamics and charged colloids. When pedestrians move relatively slowly, the typical relaxation time to adjust their velocities is negligible. In this situation, the overdamped approximation for the dynamics can be used to model the coupled motion of particles.²² In previous studies,⁶ the interaction between two pedestrians is described by a symmetrical force as,

$$f_{ij} = A \exp(r_{ij}/B) \hat{\mathbf{r}}_{ij}, \quad (5)$$

where we use $A=16.5\text{ N}$ and $B=1\text{ m}$. In higher densities of pedestrians, hard-core and friction forces need to be introduced to account for body-body contact.^{6,22} This effect, as well as the inertial term, are more relevant in situations of panic. Here, as in the case of vortices, we also measure the effective parameter a for confined geometries under mechanical equilibrium. This value is then used to fit the density profiles from molecular dynamics simulations with a piece-wise solution for Eq. (3) in the general form of Eq. (4). As shown in the inset of Fig. 7, the agreement between simulations and continuum model is rather impressive for this system.

Our continuum approach to particle flow can also be applied to the transport of charged colloidal particles. These systems are usually modeled by an interaction potential in the Yukawa's form²³

$$V_{ij} = \frac{\exp(-\kappa r_{ij})}{r_{ij}} f_0 \lambda^2, \quad (6)$$

where we have used $\kappa=0.8$ for the screening parameter. The density profiles for a system of particles interaction via Eq.

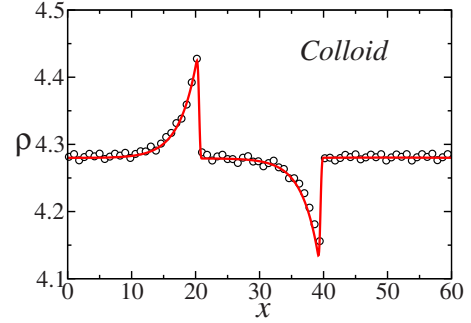


FIG. 8. (Color online) Density profile for a system of colloidal charged particles, interacting via Yukawa's potential (6), flowing across a potential barrier obstacle, as described in Fig. 3. The external applied force is $F=4.0f_0$, the potential jump is $\Delta U=1.0f_0\lambda$, the number of particles is $N=600$, and the channel width is $L=5\lambda$. In the figure we also show that the numerical integration of Eq. (3) follows closely the results obtained from molecular dynamics simulations.

(6) and passing through a obstacle barrier is shown in Fig. 8. As before the density profile can be suitably adjusted by using Eq. (3), further confirming the validity and broad-range applicability of the continuum description to model the collective motion of particles undergoing overdamped dynamics in confined and irregular channels.

IV. CONCLUSIONS

In summary, we investigated the general problem of flow of interacting particles in overdamped motion through confined geometries. Regardless of the complex geometries and boundary conditions involved, we have shown the remarkable fact that the microscopic behavior of the overdamped system is fully compatible with a continuum coarse-grained model, described in terms of a nonlinear diffusion equation. We corroborated the general validity of our theoretical approach with results for three distinct physical systems. Our results show that the quantity a , which parameterizes the effective strength of the interaction between the particles, needs to be adjusted to account for the confined geometry. We observed that for certain conditions, where the force acting on the particles varies rapidly over short distances, the theoretical predictions deviate from the results obtained for the discrete system of particles. However, it was possible to show that these deviations may be accounted for by finding the proper boundary conditions in the interface region where the external force varies. As an extension for future work, we will apply Eq. (2) to describe the behavior of more complex systems, including, for instance, stress with the walls, interactions with pinning centers, or substrates whose geometries are networks of interconnected channels as observed, for instance, in the rivers of elastic flow of interacting particles.

ACKNOWLEDGMENTS

We thank CNPq, CAPES, FUNCAP, FACEPE, and FINEP for financial support.

- ¹C. Cottin-Bizonne, J.-L. Barrat, L. Bocquet, and E. Charlaix, *Nature Mater.* **2**, 237 (2003).
- ²M. Köppl, P. Henseler, A. Erbe, P. Nielaba, and P. Leiderer, *Phys. Rev. Lett.* **97**, 208302 (2006); C. Reichhardt and C. J. Olson Reichhardt, *ibid.* **92**, 108301 (2004).
- ³G. Grüner, *Rev. Mod. Phys.* **60**, 1129 (1988); E. Slot, H. S. J. van der Zant, K. O'Neill, and R. E. Thorne, *Phys. Rev. B* **69**, 073105 (2004); K. O'Neill, E. Slot, R. E. Thorne, and H. S. J. van der Zant, *Phys. Rev. Lett.* **96**, 096402 (2006).
- ⁴J. H. Morais-Cabral, Y. Zhou, and R. Mackinnon, *Nature (London)* **414**, 37 (2001); S. Matthias and F. Müller, *ibid.* **424**, 53 (2003); R. Roth and D. Gillespie, *Phys. Rev. Lett.* **95**, 247801 (2005).
- ⁵R. Besseling, N. Kokubo, and P. H. Kes, *Phys. Rev. Lett.* **91**, 177002 (2003); C. C. de Souza Silva, L. R. E. Cabral, and J. A. Aguiar, *Physica C* **404**, 11 (2004); *Phys. Rev. B* **63**, 134526 (2001).
- ⁶D. Helbing, I. J. Farkas, and T. Vicsek, *Phys. Rev. Lett.* **84**, 1240 (2000); T. Nagatani, *Physica A* **300**, 558 (2001).
- ⁷N. Kokubo, R. Besseling, V. M. Vinokur, and P. H. Kes, *Phys. Rev. Lett.* **88**, 247004 (2002); I. V. Grigorieva, A. K. Geim, S. V. Dubonos, K. S. Novoselov, D. Y. Vodolazov, F. M. Peeters, P. H. Kes, and M. Hesselberth, *ibid.* **92**, 237001 (2004).
- ⁸G. Piacente and F. M. Peeters, *Phys. Rev. B* **72**, 205208 (2005).
- ⁹V. V. Bryksin and S. N. Dorogovtsev, *JETP* **77**, 791 (1993); *Physica C* **215**, 173 (1993).
- ¹⁰S. Zapperi, A. A. Moreira, and J. S. Andrade, Jr., *Phys. Rev. Lett.* **86**, 3622 (2001).
- ¹¹A. A. Moreira, J. A. Andrade, Jr., J. Mendes Filho, and S. Zapperi, *Phys. Rev. B* **66**, 174507 (2002); S. Zapperi, J. S. Andrade, Jr., and A. A. Moreira, *Physica A* **342**, 383 (2004).
- ¹²H. J. Jensen, A. Brass, and A. J. Berlinsky, *Phys. Rev. Lett.* **60**, 1676 (1988).
- ¹³O. Pla and F. Nori, *Phys. Rev. Lett.* **67**, 919 (1991); R. A. Richardson, O. Pla, and F. Nori, *ibid.* **72**, 1268 (1994); W. Barford, W. H. Beere, and M. Steer, *J. Phys.: Condens. Matter* **5**, L333 (1993).
- ¹⁴C. Reichhardt, C. J. Olson, J. Groth, S. Field, and F. Nori, *Phys. Rev. B* **52**, 10441 (1995); **53**, R8898 (1996).
- ¹⁵C. Reichhardt, J. Groth, C. J. Olson, S. B. Field, and F. Nori, *Phys. Rev. B* **54**, 16108 (1996); **56**, 14196 (1997).
- ¹⁶A. L. Fetter and P. C. Hohenberg, *Phys. Rev.* **159**, 330 (1967).
- ¹⁷E. H. Brandt, *Phys. Rev. B* **79**, 134526 (2009).
- ¹⁸J. Pearl, *Appl. Phys. Lett.* **5**, 65 (1964).
- ¹⁹This is the adequate expression for vortex interaction in bulk form. For the thin film case, one should use the appropriate expression. Nevertheless, as we show in the body of the article, the results are independent of the form of the interaction, as long as it is repulsive and short-ranged.
- ²⁰A. Pruyboom, P. H. Kes, E. van der Drift, and S. Radelaar, *Phys. Rev. Lett.* **60**, 1430 (1988); M. H. Theunissen, E. Van der Drift, and P. H. Kes, *ibid.* **77**, 159 (1996).
- ²¹M. Sbragaglia, R. Benzi, L. Biferale, S. Succi, and F. Toschi, *Phys. Rev. Lett.* **97**, 204503 (2006).
- ²²D. Helbing, *Rev. Mod. Phys.* **73**, 1067 (2001).
- ²³K. Kremer, M. O. Robbins, and G. S. Grest, *Phys. Rev. Lett.* **57**, 2694 (1986); P. Wette, I. Klassen, D. Holland-Moritz, T. Palberg, S. V. Roth, and D. M. Herlach, *Phys. Rev. E* **79**, 010501(R) (2009).